

Alternative polyadenylation of ABC-transporters of the C-family (ABCC1, ABCC2, ABCC3) and implications on post-transcriptional micro-RNA regulation

Oliver Bruhn^{1†}, Marie Lindsay^{1†}, Friederike Wiebel¹, Meike Kaehler¹, Inga Nagel¹,
Ruwen Böhm¹, Christian Röder², Ingolf Cascorbi^{1‡}

¹Institute of Experimental and Clinical Pharmacology, University Hospital Schleswig-Holstein, Campus Kiel, Kiel, Germany

²Institute for Experimental Cancer Research, University Hospital Schleswig-Holstein, Campus Kiel, Kiel, Germany

[†]These authors contributed equally to this work

[‡]Corresponding author

Correspondence address:

Prof. Ingolf Cascorbi, MD, PhD
Institute of Experimental and Clinical Pharmacology
Arnold-Heller-Strasse 3
24105 Kiel
Germany
Phone: +49 431-500-30400
Fax: +49 431-500-30404
E-mail: cascorbi@pharmakologie.uni-kiel.de

Short title: Alternative polyadenylation of ABCC-transporters

Number of text pages: 19

Number of tables: 3

Number of figures: 7

Number of references: 52

Number of words in the abstract: 198

Number of words in the introduction: 697

Number of words in the discussion: 1341 (1500 incl. concluding remarks)

Nonstandard abbreviations: 0

Abstract

ABC-transporters represent a large group of efflux pumps being strongly involved in the pharmacokinetics of various drugs as well as of nutrient distribution. It was recently shown that miRNAs may significantly alter their expression as proven e.g. for miR-379 and *ABCC2*. However, alternative mRNA polyadenylation may result in expression of 3'-untranslated regions (3'-UTRs) with varying lengths. Thus, length variants may result in presence or absence of miRNA binding sites for regulatory micro-RNAs with consequences on posttranscriptional control. In the present study, we report on 3'-UTR variants of *ABCC1*, *ABCC2*, and *ABCC3* mRNA. Applying *in vitro* luciferase reporter gene assays, we show that expression of short *ABCC2* 3'-UTR variants leads to a significant loss of miR-379/*ABCC2* interaction and subsequent upregulation of *ABCC2* expression. Further, we show that expression of *ABCC2* 3'-UTR lengths varies significantly between human healthy tissues, but is not directly correlated to the respective protein level *in vivo*.

Concluding, presence of altered 3'-UTR lengths in ABC-transporters could lead to functional consequences with regards to posttranscriptional gene expression potentially regulated by alternative polyadenylation. Hence, 3'-UTR length variability may be considered as a further mechanism contributing to variability of ABCC transporter expression and subsequent drug variation in drug response.

Significance statement

microRNA binding to the 3'-UTR plays an important role in control of ABC-transporter mRNA degradation and translation into proteins. We disclosed various 3'-UTR length variants of *ABCC1*, *C2* and *C3* mRNA partly with loss of mRNA seed regions leading to varying and tissue-dependent interaction with miRNAs as proven by reporter gene

assays. Alternative 3'-UTR length may contribute to variable ABCC-transporter expression and potentially explains inconsistent findings in microRNA studies.

Introduction

ATP binding cassette (ABC) transporters mediate active transport of diverse endogenous compounds, xenobiotics and drugs across barriers thereby contributing to endogenous distribution of nutrients, detoxification and drug elimination (Rees et al., 2009). Having 13 members, the C-subfamily is the largest among the seven ABC-transporter subfamilies (Moitra and Dean, 2011). Within the ABCC-subfamily, mainly ABCC1 (MRP1), ABCC2 (MRP2) and ABCC3 (MRP3) are involved in the bioavailability of various drugs influencing their absorption, distribution and elimination or restricting the permeability of blood-tissue barriers (Chen et al., 2016; Kunicka and Soucek, 2014; van der Schoor et al., 2015). Next to their contribution to drug response, *ABCC*-transporters are involved in the etiology of several human pathologies. ABCC1, transporting conjugated and unconjugated organic anions, plays a role in immunological and cardiovascular diseases, as well as neurological disorders and tumor progression (Cole 2014). ABCC2 also mediates the transport of various conjugated organic anions and is mainly responsible for the excretion of bilirubin from the bile. A genetic defect in *ABCC2* is associated with Dubin-Johnson syndrome, a recessively inherited disorder characterized by conjugated hyperbilirubinemia (van der Schoor et al., 2015). Similar to ABCC2, ABCC3 transports bile acids and organic anions, as well as numerous xenobiotics including anti-cancer drugs and acts as an alternative transporter for the export of bile acids and glucuronides from cholestatic hepatocytes. Due to the importance of these transporters in the pharmacokinetics of drugs and transport of endogenous organic anions, increased knowledge of regulatory mechanisms is of high interest.

On transcriptional level, the genes of ABCC-transporters are regulated by nuclear receptor signaling as a consequence of xenobiotic sensing and/or hormonal regulation (Kast et al., 2002; Miller, 2015). Moreover, hereditary genetic variants significantly affect transcriptional and posttranscriptional regulation and function, as shown i.e. for *ABCC2* haplotypes (Laechelt et al., 2011). In addition, ABCC-transporters underlie extensive posttranscriptional regulation through interaction with micro-RNAs (miRNAs) (Haenisch et al., 2014).

MiRNAs are small non-coding RNAs, which act through RNA-interference by forming imperfect hybrids with the 3'-UTR of their target mRNAs leading to mRNA degradation or translation inhibition (Ambros, 2001). Various miRNAs were reported to bind to the 3'-UTRs of *ABCC* mRNAs, currently nine for *ABCC1* (Hu et al., 2018; Kunicka and Soucek, 2014; Li et al., 2018a; Li et al., 2018b; Liang et al., 2010; Liu et al., 2015; Ma et al., 2015; Pan et al., 2013; Pei et al., 2016; Sun et al., 2017), four for *ABCC2* (Haenisch et al., 2011; He et al., 2017; Tian et al., 2017; Zhan et al., 2013), and two for *ABCC3* (An et al., 2018; Bruckmueller et al., 2017). Functional confirmation of miRNA binding was predominantly executed by reporter-gene assays, i.e. binding of miRNA-379 to the *ABCC2* 3'-UTR (Haenisch et al., 2011). However, alternative polyadenylation was not considered in these studies.

Alternative polyadenylation is an RNA-processing mechanism generating mRNAs with distinct 3'-UTR lengths. Being widespread across all eukaryotic species, it is considered as a major mechanism of gene regulation (Tian and Manley, 2017). About 50-75 % of all human genes underlie alternative polyadenylation resulting in multiple possible poly-A-sites of one respective mRNA (Shi, 2012; Tian et al., 2005). Moreover, more than 50 % of conserved miRNA target sites in the 3'-UTRs are affected by alternative polyadenylation (Sandberg et al., 2008). Furthermore, alternative polyadenylation is tissue specific and an important determinant for protein synthesis.

Thereby, it plays a role in cell proliferation and differentiation, as well as cancer cell progression (Mayr, 2016; Mayr and Bartel, 2009). Several studies observed that ABC-transporters are substantially affected by alternative polyadenylation. For ABCB1 (P-glycoprotein) and ABCG2 (BCRP), it was shown that alternative polyadenylation influences their posttranscriptional regulation and protein synthesis subsequently contributing to pharmacoresistances of cancer cells (Bruhn et al., 2016; To et al., 2009). Despite their importance in drug disposition, nutrient transport and health, the extent of alternative polyadenylation in ABCC-transporters remains unknown. The present study aimed to determine alternative polyadenylation of the ABC-transporters *ABCC1*, *ABCC2*, and *ABCC3* and to investigate its potential regulatory implications, if 3'-UTR shortening leads to loss of miRNA binding sites and respective miRNA binding. Furthermore, the expression of different *ABCC2* 3'-UTR variants in human liver, colon, and gall bladder tissues were analyzed and compared to *ABCC2* protein levels.

Materials and Methods

Cell cultivation

HepG2, SK-Hep-1, and Caco-2 cells were purchased from the German Collection of Microorganisms and Cell Cultures (DSMZ, Braunschweig, Germany). HepG2 cells were grown in RPMI1640 medium (PAA, Pasching, Germany), supplemented with 10 % v/v heat-inactivated fetal bovine serum (FBS, PAA) and 1 % v/v penicillin (10,000 U/ml)/streptomycin (10 mg/ml) (P/S; PAA), SK-Hep-1 cells were grown in RPMI1640 medium supplemented with 20 % v/v FBS and 1 % v/v P/S, Caco-2 cells were grown in DMEM medium (with L-glutamine and 4.5 g/l glucose) (PAA) supplemented with 10 % v/v FBS enriched with 1 % v/v non-essential amino-acids (PAA) and 1 % v/v P/S. Medium was replaced and cells were passaged every 2 or 3

days, depending on the cell density. For RNA extraction, 5×10^6 cells were solubilized in 600 μ l RLT-buffer (Qiagen, Hilden, Germany) supplemented with 1 % v/v β -mercaptoethanol (Roth, Karlsruhe, Germany) and homogenized using a rotor-stator homogenizer (Polytron PT 3000, Kinematica AG, Littau, Switzerland). The RNA was extracted using the RNeasy Mini Kit (Qiagen) according to the manufacturer's specifications. Prior to reverse transcription, residual DNA was digested using the Turbo DNA-free™ Kit (Ambion, Austin, USA) according to the manufacturer's specifications.

Human tissue samples

Human tissue samples (liver, colon and gall bladder) were obtained from patients undergoing tumor surgery at the University Hospital Schleswig-Holstein, Campus Kiel (Tab. 1). Patients gave their written informed consent, and the study was approved by the ethics committee of the Medical Faculty of the University of Kiel. Specimen of non-malignant peritumoral tissue were obtained from the resectate after verification by a pathologist and were stored over night at 4 °C in RNAlater reagent (Qiagen), prior to long-term storage at -80 °C. Tissue RNA was extracted using the Precellys 24 Tissue Homogenizer applying Precellys ceramic beads (1.4 mm) tubes (PEQLAB, Erlangen, Germany) and the RNeasy Mini Kit (Qiagen) according to the manufacturer's specifications.

Reverse transcription

5 μ g total RNA were reversely transcribed using the SuperScript II reverse transcriptase (Invitrogen, Carlsbad, USA) and the poly-dT-Primer QT (Tab. 2) according to the protocol of Scotto-Lavino et al. (Scotto-Lavino et al., 2006). Residual

RNA-fragments were digested using RNase H (Invitrogen) and the generated cDNA was diluted with 75 μ l TE-buffer (Tris-EDTA, Roth).

Primer generation, 3'-RACE reaction and purification of PCR-products

All gene-specific forward primers were generated using the Primer-BLAST online tool with standard settings (<https://www.ncbi.nlm.nih.gov/tools/primer-blast/>) based on the NCBI *ABCC1/2/3* sequences (NM_004996.3, NM_000392.4, and NM_003786.3). A schematic representation of primers used in the present study is shown in Fig. 1, primer specifications and sequences are shown in Tab. 2. 3'-RACE reactions were performed in a two-step procedure according to the protocol of Scotto-Lavino using various primer combinations as shown in Fig. 1 (Scotto-Lavino et al., 2006). In a first amplification round, gene-specific forward primers with binding site upstream the stop codon in combination with the QO reverse primer, complementary to a rear artificial tail located at the 3'-end of the cDNA generated by the QT poly-dT primer, were used. In a second amplification round, diluted amplification products (1:20 in TE-buffer) of the first round were used as template in a nested PCR approach. For this, gene-specific forward primers binding downstream the forward primers used for the first amplification round were combined with R-QI primers, complementary to the anterior artificial end of the cDNA 3'-end. A schematic representation of all 3'-RACE reactions is shown in Fig. 1. All experiments were performed on a GeneAmp[®] PCR system 9700 (Applied Biosystems, Darmstadt, Germany) using the HotStarTaq[®] Master Mix Kit (Qiagen). All products used for sequencing were purified by gel electrophoresis (1.5 % w/v agarose, supplemented with 1 mM guanosine) and subsequent gel extraction using the QIAquick Gel Extraction Kit (Qiagen) according to the manufacturer's recommendations.

Sequencing and sequence analysis

PCR-products were verified by Sanger sequencing at the Institute of Clinical Molecular Biology of the University Hospital Kiel, Campus Kiel, Germany. Obtained sequences were analyzed and aligned using the BioEdit Sequence Alignment Editor version 7.2.6 (URL: <http://www.mbio.ncsu.edu/BioEdit/>).

Quantitative Real-Time PCR (qRT-PCR)

To quantify different *ABCC2* 3'-UTR lengths present in the human tissue samples, qRT-PCR experiments were performed, applying three different primer combinations (Tab. 2) with binding sites in distinct *ABCC2* 3'-UTR isoforms (Fig. 5) using the SYBR Green SYBR[®] Select[™] Master Mix (Applied Biosystems) on an ABI Prism 7900 HT Sequence Detection System (Applied Biosystems). Relative 3'-UTR amount was calculated by normalization with β -actin.

Luciferase reporter-gene assays

Primers to amplify the *ABCC2* 3'-UTR variants with 178 bp/429 bp/944 bp were generated using the TaKaRa In-Fusion Cloning primer designing tool (TaKaRa Bio Group; <https://www.takarabio.com/learning-centers/cloning/in-fusion-cloning-tools>) and PCR products were amplified with the forward primer F_{hd} (5'-GCTCGCTAGCCTCGAGCTGGCATTGAGAATGTGAA-3') combined with the reverse primers R_{hd178} (5'-CGACTCTAGACTCGACAATCGAGGGGTTTCTC-3'), R_{hd429} (5'-CGACTCTAGACTCGATGCACCTATTTGCATCACCA-3'), and R_{hd944} (5'-CGACTCTAGACTCGAAAAATTCAAGACATAACAAGGAA-3') using the HotStarTaq[®] Master Mix Kit (Qiagen). The pmirGLO dual luciferase vector (Promega, Mannheim, Germany) was digested overnight with the restriction enzyme *Xho* I (NEB, Ipswich, MA, USA). Amplicons were cloned into the pmirGLO vector using the In-

Fusion® HD Cloning Kit (Takara Bio, USA) according to the manufacturer specifications. Correct insertion and orientation of the amplicons into the vector was confirmed by Sanger sequencing. 10^5 HepG2 cells were co-transfected with 100 ng of the target-vector or empty control-vector and 10/25/50 nM of hsa-miR-379-5p Pre-miR™ miRNA Precursor (PM10316, Thermo Fisher Scientific, Germany) using the siPORT NeoFX transfection agent (Ambion). Pre-miR micro-RNA precursor negative control #1 (AM17110, Thermo Fisher) served as negative control. 48 hours after transfection, HepG2 cells were lysed and firefly and renilla luciferase activity was measured using the Dual-Luciferase® Reporter Assay System (Promega) and a Veritas microplate luminometer (Turner Biosystems, CA, USA). Firefly luciferase activity was normalized to renilla luciferase activity (internal standard), and normalized firefly luciferase activity obtained with pre-miR-379 was compared with the activity obtained with the pre-miR negative control.

Immunoblotting

Human tissue samples were cut into 15 μ m slices using the CryoStar NX50 (Thermo Fisher), collected into Precellys-Tubes with 2.8 mm ceramic beads and homogenized at 6000 rpm for 20 s in the Precellys homogenizer (VWR) in 500 μ l RIPA buffer supplemented with 0.2 % w/v BSA. Subsequent lysis was performed by sonication for 13 s. Enrichment of membrane proteins was accomplished using the Plasma Membrane Protein Extraction Kit (Abcam, Berlin, Germany) with 500 μ l Homogenize Buffer Mix according to the manufacturer's protocol. Protein quantification and Western blotting were executed according to standard protocols as previously described (Waetzig et al. 2019). Blots were probed with the following antibodies: ABCC2: Santa Cruz Biotechnology Cat# sc-518048, dilution 1:100; GAPDH: Santa Cruz Biotechnology Cat# sc-47724, dilution 1:5000; anti-mouse: LiCOR IRDye 800CW Cat#

926-32210, dilution 1:10,000. Primary antibodies were diluted in Odyssey Blocking Solution, secondary antibodies in TBS with 0.2 % v/v Tween. Blots were visualized using the Odyssey CLx imager (LiCOR, Bad Homburg, Germany). Densitometry was performed using Empiria Studio Software 1.1 (LiCOR).

Results

3'-RACE and agarose gel electrophoresis

Using HepG2, SK-Hep-1 or Caco-2 mRNA as templates, numerous amplicons of *ABCC1*, *ABCC2* and *ABCC3* mRNAs were generated using various forward primers combined with the reverse primers QO and/or QI (Fig. 1, Tab. 2). Some of the primer combinations generated side products with either no sequence homologies to *ABCC1*, *ABCC2* or *ABCC3*, or to products, which have been unevaluable due to sequence overlays (black arrows, Fig. 2), or having the expected 3'-UTR sequence, but no detectable poly-A-tail. However, the majority of primer combinations, especially for *ABCC2* and *ABCC3*, led to PCR products with evaluable 3'-UTR sequences, required for exact determination of 3'-UTR variants (white arrows, Fig. 2). Most of the products were generated by the second amplification round (Fig. 2A, right gel; Fig. 2B; Fig. 2C, middle and right gel), only few products were directly evaluable after sequencing of the first amplification round (Fig. 2A, left gel; Fig 2C, left gel). All evaluable sequences with detectable poly-A-tails at the 3'-UTR ends were analyzed. The obtained consensus sequences are shown in Supplementary Fig. 1. No detectable amplicons were generated with the forward-primers *ABCC1_Fgen6629*, *ABCC1_Fgen6674*, *ABCC1_Fgen6727*, and *ABCC3_Fgen6105*, *ABCC3_Fgen6107*, *ABCC3_Fgen6193* (Tab. 2, Fig. 1), as sufficiently long 3'-UTR sequences were missing. The *ABCC1* forward-primers *ABCC1_F4884*, *ABCC1_F4943*, and *ABCC1_F5074* (Tab. 2, Fig. 1) generated products homologous to the *ABCC1* 3'-UTR, but with no detectable poly-A-

tail indicating no further 3'-UTR variants between the two observed *ABCC1* 3'-UTRs. For *ABCC2*, five different 3'-UTR variants and four 3'-UTR variants for *ABCC3* were identified.

Determination of mRNA 3'-UTR lengths in ABCC1, ABCC2, and ABCC3

ABCC1

According to the NCBI reference sequence NM_004996.3, the *ABCC1* gene consists of 6,564 bp with a coding sequence of 4,595 bp. The *ABCC1* 3'-UTR starts at position 4772 after the TGA stop codon and has a length of 1793 bp ending at position 6564 (poly-A site). However, our 3'-RACE experiments on cDNA from hepatoblastoma and colon carcinoma cell lines demonstrated that *ABCC1* is expressed with two different mRNA 3'-UTRs, a short one of 105 bp (counted from the first base downstream the stop codon up to the last base upstream the poly-A-tail) and one markedly prolonged 3'-UTR of 1,771 bp (Fig. 3). A 3'-UTR of 1,793 bp, as noted in the NCBI database, could not be confirmed in our study.

ABCC2

According to the latest version in the NCBI database the *ABCC2* gene spans 5,806 bp with a coding sequence of 4,637 bp. No polyadenylation signals or polyadenylation sites are noted in the database. The *ABCC2* consensus sequence resulting from our 3'-RACE experiments was identical with the sequence of the NCBI database entry. Nevertheless, the last 22 nucleotides of the NCBI sequence, denoted as part of exon 31, were not present in the 3'-UTRs identified in this study. Overall, a total of five different 3'-UTRs with lengths of 178 bp, 363 bp, 429 bp, 840 bp, and 944 bp, respectively, were discovered (Fig. 3).

ABCC3

Twelve different putative mRNA 3'-UTRs for *ABCC3* are listed in the NCBI AceView database, ranging from 46 to 2077 bp (spliced mRNA variants). It should be noted that two different gene variants exist for *ABCC3*. According to the NCBI database, variant 1 encodes the longer isoform (NM_003786.3), whereas variant 2 lacks multiple 3' exons, has an alternative 3' sequence and the resulting isoform is much shorter with a different C-terminus (NM_001144070.1). However, as the fully functional *ABCC3* transporter is based on variant 1 (isoform NM_003786.3), the present study refers only to this variant. In the NCBI nucleotide database, the *ABCC3* entry (NM_003786.3) has a 3'-UTR length of 502 bp with the most common AATAAA polyadenylation signal 24 bp upstream of the polyadenylation site. This 3'-UTR was confirmed in the present study. In addition, three alternative 3'-UTR variants were identified for *ABCC3* with lengths of 306 bp, 1053 bp, and 1,427 bp, respectively (Fig. 3).

Functional verification

To prove the concept that miRNA-mediated posttranscriptional regulation is dependent on alternative polyadenylation and can be impaired by shortening of the respective 3'-UTR, we cloned three *ABCC2* 3'-UTR variants (178 bp, 429 bp, and 944 bp long 3'-UTRs) in a luciferase vector and co-transfected the respective vector constructs along with miR-379 in HepG2 cells. As expected, the shortest variant (178 bp) was not regulated by miR-379, whereas the longer variants (429 bp and 944 bp) both showed a significant reduction of reporter-gene expression in the presence of miR-379 (Fig. 4). These results confirm the influence of alternative polyadenylation on the posttranscriptional regulation of *ABCC2* through miR-379.

Distribution of ABCC2 3'-UTR variants in human tissue

The distribution of the three *ABCC2* mRNA 3'-UTR variants (178, 363, 840 bp) were investigated in human peritumoral non-malignant liver, gall bladder, and colon tissues by qRT-PCR using SYBRGreen® and primer combinations with binding sites within the respective 3'-UTR generating amplicons with approximately equal lengths (Fig. 5). Taken into account that the primer pair 1 binds to all possible 3'-UTRs, primer combination 2 to the 363/429/840/944 bp variants and primer combination 3 to the two longest 3'-UTRs (840 and 944 bp) the results show that the long 3'-UTR variants (840 bp and 944 bp *ABCC2* 3'-UTR isoforms) are predominantly expressed in the liver sample compared to colon ($p=0.03$) or gall bladder ($p=0.04$).

ABCC2 protein quantification

Western blotting revealed that only the liver samples exhibit a consistent *ABCC2* protein synthesis (Fig. 6). Four of the five analyzed gall bladder samples show a minor but detectable *ABCC2* abundance, whereas there was lack of *ABCC2* protein within the colon samples. Calculation of the mean intensity optical densitometry (IOD) of the bands confirmed significant *ABCC2* synthesis in the liver samples, absence of *ABCC2* protein in the colon samples and marginal *ABCC2* synthesis in the gall bladder.

Discussion

Alternative polyadenylation occurs in the majority of eukaryotic cells and is an important regulatory mechanism of gene expression (Tian and Manley, 2013). The 3'-UTR of mRNAs serves as a major regulatory region for trans-acting factors controlling stability, cellular localization and translation efficiency of the target mRNAs (Elkon et al., 2013). The latter is especially true for miRNAs. The importance of alternative polyadenylation was shown for various biological processes including cell

development, differentiation and proliferation (Carpenter et al., 2014; Elkon et al., 2013; Jia et al., 2017). Widespread 3'-UTR shortening by alternative polyadenylation was reported in cancer cell development leading to oncogene activation (Mayr and Bartel, 2009). Alternative polyadenylation occurs also in ABC-transporters, as reported for ABCB1 (Bruhn et al., 2016) and ABCG2 (To et al., 2009), both highly relevant for drug bioavailability contributing to anti-cancer drug-resistance (Fohner et al., 2017; Yakusheva and Titov, 2018). Besides ABCG2 and ABCB1, ABC-transporters of the C-family, especially ABCC1, ABCC2 and ABCC3, are relevant for pharmacokinetics as well as internal nutrient distribution. Due to their biological importance, it is essential to understand the regulation of these transporters and the extent of alternative polyadenylation they underlie. Here, we identified two different 3'-UTR length variants in *ABCC1* mRNA, five in *ABCC2*, and four in *ABCC3*.

A comparison of the resulting *ABCC1* mRNA sequence with the NCBI database entry revealed no sequence varieties, except for the last 22 bp of the 3'-UTR, which are absent in the consensus sequence. The *ABCC1* 3'-UTR starts with a GCC-triplet downstream the TGA stop codon. A TATATC motif at the end of the 1,771 bp variant and an ACCAAA motif at the end of the short 105 bp 3'-UTR was observed. Potential polyadenylation signals for the short *ABCC1* 3'-UTR might be GCCTCC or CCTCCC located 22 or 21 nucleotides upstream the poly-A-tail (Gruber et al., 2016). However, these are rare polyadenylation signals in eukaryotes, which are not experimentally confirmed. For the long 3'-UTR, potential polyadenylation sites are TAAAAA, AAAAAT or AAAATA (21, 17 and 16 nucleotides upstream the poly-A-tail). Three different *ABCC1* 3'-UTR fragments were previously described in the experimental NCBI AceView-Database (aAug10-gAug10) with lengths of 1,793, 244 and 227 bp. Compared with the present analysis, these entries could not be confirmed despite the usage of 12 different forward primers for the 3'-RACE experiments.

The shortest *ABCC2* 3'-UTR is 178 bp long and has a common AATAAA polyadenylation signal 23 nucleotides upstream of the polyadenylation site (Gruber et al., 2016; Tian et al., 2005). The 363 bp 3'-UTR has putative polyadenylation sites 36 and 38 bp upstream (TTTTTT and CCTTTT) the polyadenylation site, the 429 bp 3'-UTR has three potential polyadenylation signals (TTCTTT, TCTTTT, and TTTTGT) 47, 46, and 44 nucleotides upstream the polyadenylation site being rare in eukaryotes (Gruber et al., 2016). The putative polyadenylation signals of the 840 and 944 bp *ABCC2* 3'-UTRs are more common. These are TTTTTT or TTTAAA for the 840 bp 3'-UTR, 30 and 27 nucleotides upstream the poly-A-site, and TTTTAA or TTTATT (28 and 26 nucleotides upstream the poly-A-site) for the 944 bp fragment. The AceView database reveals six entries for *ABCC2* 3'-UTR variants (13, 56, 292, 750 and 945 bp). Only the 945 bp fragment (944 bp in the present study) was confirmed. Neither the short *ABCC2* 3'-UTRs variants with a length of 13 or 56 bp, nor the 292 or 750 bp long variants were found.

Except for the 502 bp 3'-UTR, *ABCC3* entries in AceView were not confirmed. The 306 bp *ABCC3* 3'-UTR variant found here has a common polyadenylation signal (AAATAA) 22 nucleotides upstream the poly-A tail. In contrast, the 1,053 and 1,427 bp variants have rare polyadenylation signals, potentially ATTAAA for the 1,053 bp 3'-UTR (28 nucleotides upstream the polyadenylation site) and ATAAAG for the 1,427 bp fragment, 24 nucleotides upstream the polyadenylation site. The *ABCC3* 3'-UTR starts with an AAT-triplet following the TAA stop codon.

Various miRNAs were identified to bind to the 3'-UTR of the three *ABCC* transporters (Tab. 3). It should be noted that for three of them (miR-9 for *ABCC1*, miR-205-5p for *ABCC2* and miR-143 for *ABCC3*) the reported miRNA binding sites are not present in the current NCBI mRNA sequence entries. However, the majority of miRNAs have binding sites located in prolonged 3'-UTRs of *ABCC1*, *ABCC2* and *ABCC3*, but not in

the short 3'-UTR variants. Thus, these micro-RNAs might be affected by alternative polyadenylation and their binding sites disappear when shortening of the respective 3'-UTR occurs. As a consequence, the posttranscriptional downregulation of expression may be reduced resulting in higher protein synthesis. Hence, likewise for ABCG2 (To et al., 2009) or ABCB1 (Bruhn et al., 2016), the variation of 3'-UTR lengths in members of the *ABCC*-family may also contribute to the disparity of tissue expression, as exemplified here for *ABCC2* by performing reporter-gene assays, revealing an impaired miRNA interaction and subsequent impact on gene expression dependent on the 3'-UTR length. Whereas the expression of the short *ABCC2* 178 bp 3'-UTR was not affected in the reporter gene assay, the longer 429 bp and 944 bp 3'-UTRs were down-regulated when co-transfected with miR-379, a miRNA binding to the *ABCC2* 3'-UTR as proven before by our group (Haenisch et al., 2011). In this earlier study, we verified the binding of miRNA-379 to the *ABCC2* 3'-UTR and a miRNA-379-dependent regulation of *ABCC2* mRNA and protein. Here, we observed that miRNA-379-dependent regulation of *ABCC2* 3'UTR is lost by presence of shortened 3'UTR lengths. This shows that the *ABCC2* mRNA may lose posttranscriptional control through alternative polyadenylation by 3'-UTR shortening. Hence, a possibly higher *ABCC2* protein content may contribute to altered drug response.

The importance of *ABCC2* in pharmacokinetics underlines the need for a better understanding of its regulation due to its numerous substrates, i.e. cytostatics and antibiotics (Bruhn and Cascorbi, 2014; Nies and Keppler, 2007). According to the extent of possible *ABCC2* 3'-UTR variants shown in the present study, alternative polyadenylation must be taken into account as one of the major regulation mechanisms of *ABCC2*. Here, only one miRNA-interference was analyzed, but it confirmed the hypothesis, that the shorter the 3'-UTR is, the lower is the miRNA-dependent suppression of mRNA expression. Further mRNA/miRNA interactions of ABC-

transporters should be performed to analyze the extent of posttranscriptional regulation of these important transport proteins.

By performing qRT-PCR experiments, we observed a higher amount of prolonged *ABCC2* 3'-UTRs in the liver compared to gall bladder and colon. These findings suggest a high likelihood of miRNA-mediated posttranscriptional *ABCC2* control in the liver and - in comparison - a potentially reduced regulation in gall bladder and colon. It must be taken into account that all tissue samples were obtained from cancer patients undergoing tumor surgery with a possibly changed homeostatic state of the respective site. It was observed that *ABCC2* and *ABCG2* expression was altered in moderate dysplasia in colorectal carcinogenesis suggesting an involvement of ABC-transporters in early carcinogenesis (Andersen et al., 2015). Alternative polyadenylation may contribute to *ABCC2* expression changes in colorectal carcinogenesis (Mayr and Bartel, 2009).

Immunoblotting revealed the highest *ABCC2* protein abundance in the liver, minor *ABCC2* protein in the gall bladder and almost no detectable *ABCC2* protein in the colon. The high amount in the liver is in line with the role of hepatic *ABCC2* as an efflux pump to extrude xenobiotics or metabolites, i.e. bilirubin conjugates (König et al., 1999; Cascorbi 2006). Nevertheless, *ABCC2* is known to be low expressed in the colon compared to the small intestine and underlies a large inter-individual variation (Berggren et al. 2007). In gall bladder, *ABCC2* is detectable, but up-regulated in gall bladder carcinoma (Kim et al. 2013). Here, qRT-PCR analysis of *ABCC2* 3'-UTR length polymorphisms in tissue samples revealed long *ABCC2* 3'-UTR variants in the liver. However, the observation of long 3'-UTRs in liver tissue does not imply a down-regulation *in vivo*, but potentially mirrors an important mechanism for miRNA-mediated fine-tuning of posttranscriptional gene expression. This suggests that the tissue abundance of ABC-transporters does not necessarily reflect 3'-UTR lengths and/or

miRNA interactions, but is mainly defined by other regulatory mechanisms, i.e. transcription factor expression.

Concluding remarks

The aim of our study was to identify 3'-UTR lengths of three members of the ABCC transporter family and its functional implications. First, we identified 3'-UTR length polymorphisms for *ABCC1*, *ABCC2* and *ABCC3*. In addition, the functional significance of 3'-UTR length variants on miRNA-binding were shown for *ABCC2*.

Regarding cell type, cell line or cellular status-dependent alterations in alternative polyadenylation, this might explain conflicting results in miRNA studies. Therefore, alternative polyadenylation must be taken into account, when analyzing miRNAs or miRNA/target gene-interactions. This is also true for widely used ready-to-use plasmids applied in reporter-gene assays representing only limited possibilities in observing posttranscriptional regulation.

The multitude of different 3'-UTR variants found for *ABCB1*, *ABCG2* and members of the *ABCC*-family suggest that besides transcriptional control, alternative polyadenylation is a regulatory mechanism of protein synthesis. Alternative polyadenylation should also be taken into account in pharmacogenetic studies of ABC-transporters in particular in malignant tissue exhibiting wide variation in miRNA expression profiles.

Acknowledgements

We thank Britta Schwarten for her excellent technical assistance.

Authorship Contributions

Participated in research design: Bruhn, Cascorbi, Lindsay

Conducted experiments: Bruhn, Kaehler, Lindsay, Nagel, Wiebel

Contributed to sample preparation: Bruhn, Kaehler, Lindsay, Nagel, Röder

Performed data analysis: Böhm, Bruhn, Kaehler, Lindsay, Nagel

Wrote or contributed to the writing of the manuscript: Bruhn, Cascorbi, Kaehler, Lindsay, Nagel

Footnotes

This work was supported by the Werner und Klara Kreitz-Stiftung Kiel.

References

- Ambros V (2001) microRNAs: tiny regulators with great potential. *Cell* 107(7):823-826.
- An Q, Zhou L and Xu N (2018) Long noncoding RNA FOXD2-AS1 accelerates the gemcitabine-resistance of bladder cancer by sponging miR-143. *Biomed Pharmacother* 103:415-420.
- Andersen V, Vogel LK, Kopp TI, Saebo M, Nonboe AW, Hamfjord J, Kure EH and Vogel U (2015) High ABCC2 and low ABCG2 gene expression are early events in the colorectal adenoma-carcinoma sequence. *PLoS One* 10(3):e0119255.
- Berggren S, Gall C, Wollnitz N, Ekelund M, Karlbom U, Hoogstraate J, Schrenk D, and Lennernäs H (2007) Gene and protein expression of P-glycoprotein, MRP1, MRP2, and CYP3A4 in the small and large human intestine. *Mol Pharm* 4(2):252-7.
- Bruckmueller H, Martin P, Kahler M, Haenisch S, Ostrowski M, Drozdik M, Siegmund W, Cascorbi I and Oswald S (2017) Clinically Relevant Multidrug Transporters Are Regulated by microRNAs along the Human Intestine. *Mol Pharm* 14(7):2245-2253.
- Bruhn O and Cascorbi I (2014) Polymorphisms of the drug transporters ABCB1, ABCG2, ABCC2 and ABCC3 and their impact on drug bioavailability and clinical relevance. *Expert Opin Drug Metab Toxicol* 10(10):1337-1354.
- Bruhn O, Drerup K, Kaehler M, Haenisch S, Roder C and Cascorbi I (2016) Length variants of the ABCB1 3'-UTR and loss of miRNA binding sites: possible consequences in regulation and pharmacotherapy resistance. *Pharmacogenomics* 17(4):327-340.
- Carpenter S, Ricci EP, Mercier BC, Moore MJ and Fitzgerald KA (2014) Post-transcriptional regulation of gene expression in innate immunity. *Nat Rev Immunol* 14(6):361-376.

- Cascorbi I (2006) Role of pharmacogenetics of ABC transporters in the pharmacokinetics of drugs. *Pharmacol Ther* 112: 457-473.
- Chen M, Li D, Gong N, Wu H, Su C, Xie C, Xiang H, Lin C and Li X (2017) miR-133b down-regulates ABCC1 and enhances the sensitivity of CRC to anti-tumor drugs. *Oncotarget* 8(32):52983-52994.
- Chen Z, Shi T, Zhang L, Zhu P, Deng M, Huang C, Hu T, Jiang L and Li J (2016) Mammalian drug efflux transporters of the ATP binding cassette (ABC) family in multidrug resistance: A review of the past decade. *Cancer Lett* 370(1):153-164.
- Cole SP (2014) Multidrug resistance protein 1 (MRP1, ABCC1), a "multitasking" ATP-binding cassette (ABC) transporter. *J Biol Chem* 289(45):30880-30888.
- Elkon R, Ugalde AP and Agami R (2013) Alternative cleavage and polyadenylation: extent, regulation and function. *Nat Rev Genet* 14(7):496-506.
- Fohner AE, Brackman DJ, Giacomini KM, Altman RB and Klein TE (2017) PharmGKB summary: very important pharmacogene information for ABCG2. *Pharmacogenet Genomics* 27(11):420-427.
- Gruber AJ, Schmidt R, Gruber AR, Martin G, Ghosh S, Belmadani M, Keller W and Zavolan M (2016) A comprehensive analysis of 3' end sequencing data sets reveals novel polyadenylation signals and the repressive role of heterogeneous ribonucleoprotein C on cleavage and polyadenylation. *Genome Res* 26(8):1145-1159.
- Haenisch S, Laechelt S, Bruckmueller H, Werk A, Noack A, Bruhn O, Remmler C and Cascorbi I (2011) Down-regulation of ATP-binding cassette C2 protein expression in HepG2 cells after rifampicin treatment is mediated by microRNA-379. *Mol Pharmacol* 80(2):314-320.
- Haenisch S, Werk AN and Cascorbi I (2014) MicroRNAs and their relevance to ABC transporters. *Br J Clin Pharmacol* 77(4):587-596.

- He B, Bai Y, Kang W, Zhang X and Jiang X (2017) LncRNA SNHG5 regulates imatinib resistance in chronic myeloid leukemia via acting as a CeRNA against MiR-205-5p. *Am J Cancer Res* 7(8):1704-1713.
- Hu H, Yang L, Li L and Zeng C (2018) Long non-coding RNA KCNQ1OT1 modulates oxaliplatin resistance in hepatocellular carcinoma through miR-7-5p/ ABCC1 axis. *Biochem Biophys Res Commun.* 503(4):2400-2406.
- Jia X, Yuan S, Wang Y, Fu Y, Ge Y, Lan X, Feng Y, Qiu F, Li P, Chen S and Xu A (2017) The role of alternative polyadenylation in the antiviral innate immune response. *Nat Commun* 8:14605.
- Kast HR, Goodwin B, Tarr PT, Jones SA, Anisfeld AM, Stoltz CM, Tontonoz P, Kliewer S, Willson TM and Edwards PA (2002) Regulation of multidrug resistance-associated protein 2 (ABCC2) by the nuclear receptors pregnane X receptor, farnesoid X-activated receptor, and constitutive androstane receptor. *J Biol Chem* 277(4):2908-2915.
- Kim HS, Kim NC, Chae KH, Kim G, Park WS, Park YK and Kim YW (2013). Expression of multidrug resistance-associated protein 2 in human gallbladder carcinoma. *Biomed Res Int* 2013:527534.
- König J, Nies AT, Cui Y, Leier I and Keppler D (1999) Conjugate export pumps of the multidrug resistance protein (MRP) family: localization, substrate specificity, and MRP2-mediated drug resistance. *Biochim Biophys Acta.* 1461(2):377-94.
- Kunicka T and Soucek P (2014) Importance of ABCC1 for cancer therapy and prognosis. *Drug Metab Rev* 46(3):325-342.
- Laechelt S, Turrini E, Ruehmkorf A, Siegmund W, Cascorbi I and Haenisch S (2011) Impact of ABCC2 haplotypes on transcriptional and posttranscriptional gene regulation and function. *The pharmacogenomics journal* 11(1):25-34.

- Li S, Yang J, Wang J, Gao W, Ding Y and Jia Z (2018a) Down-regulation of miR-210-3p encourages chemotherapy resistance of renal cell carcinoma via modulating ABCC1. *Cell Biosci* 8:9.
- Li Y, Liu Y, Ren J, Deng S, Yi G, Guo M, Shu S, Zhao L, Peng Y and Qi S (2018b) miR-1268a regulates ABCC1 expression to mediate temozolomide resistance in glioblastoma. *J Neurooncol*. 138(3):499-508.
- Liang Z, Wu H, Xia J, Li Y, Zhang Y, Huang K, Wagar N, Yoon Y, Cho HT, Scala S and Shim H (2010) Involvement of miR-326 in chemotherapy resistance of breast cancer through modulating expression of multidrug resistance-associated protein 1. *Biochem Pharmacol* 79(6):817-824.
- Liu H, Wu X, Huang J, Peng J and Guo L (2015) miR-7 modulates chemoresistance of small cell lung cancer by repressing MRP1/ABCC1. *Int J Exp Pathol* 96(4):240-247.
- Ma J, Wang T, Guo R, Yang X, Yin J, Yu J, Xiang Q, Pan X, Tang H and Lei X (2015) Involvement of miR-133a and miR-326 in ADM resistance of HepG2 through modulating expression of ABCC1. *J Drug Target* 23(6):519-524.
- Mayr C (2016) Evolution and Biological Roles of Alternative 3'UTRs. *Trends Cell Biol* 26(3):227-237.
- Mayr C and Bartel DP (2009) Widespread shortening of 3'UTRs by alternative cleavage and polyadenylation activates oncogenes in cancer cells. *Cell* 138(4):673-684.
- Miller DS (2015) Regulation of ABC transporters at the blood-brain barrier. *Clin Pharmacol Ther* 97(4):395-403.
- Moitra K and Dean M (2011) Evolution of ABC transporters by gene duplication and their role in human disease. *Biol Chem* 392(1-2):29-37.

- Nies AT, Keppler D (2007) The apical conjugate efflux pump ABCC2 (MRP2). *Pflugers Arch* 453(5):643-59.
- Pan YZ, Zhou A, Hu Z and Yu AM (2013) Small nucleolar RNA-derived microRNA hsa-miR-1291 modulates cellular drug disposition through direct targeting of ABC transporter ABCC1. *Drug Metab Dispos* 41(10):1744-1751.
- Pei K, Zhu JJ, Wang CE, Xie QL and Guo JY (2016) MicroRNA-185-5p modulates chemosensitivity of human non-small cell lung cancer to cisplatin via targeting ABCC1. *Eur Rev Med Pharmacol Sci* 20(22):4697-4704.
- Rees DC, Johnson E and Lewinson O (2009) ABC transporters: the power to change. *Nat Rev Mol Cell Biol* 10(3):218-227.
- Sandberg R, Neilson JR, Sarma A, Sharp PA and Burge CB (2008) Proliferating cells express mRNAs with shortened 3' untranslated regions and fewer microRNA target sites. *Science* 320(5883):1643-1647.
- Scotto-Lavino E, Du G and Frohman MA (2006) 3' end cDNA amplification using classic RACE. *Nat Protoc* 1(6):2742-2745.
- Shi Y (2012) Alternative polyadenylation: new insights from global analyses. *RNA* 18(12):2105-2117.
- Sun J, Zhang H, Li L, Yu L and Fu L (2017) MicroRNA-9 limits hepatic fibrosis by suppressing the activation and proliferation of hepatic stellate cells by directly targeting MRP1/ABCC1. *Oncol Rep* 37(3):1698-1706.
- Tian B, Hu J, Zhang H and Lutz CS (2005) A large-scale analysis of mRNA polyadenylation of human and mouse genes. *Nucleic Acids Res* 33(1):201-212.
- Tian B and Manley JL (2013) Alternative cleavage and polyadenylation: the long and short of it. *Trends Biochem Sci* 38(6):312-320.
- Tian B and Manley JL (2017) Alternative polyadenylation of mRNA precursors. *Nat Rev Mol Cell Biol* 18(1):18-30.

- Tian J, Xu YY, Li L and Hao Q (2017) MiR-490-3p sensitizes ovarian cancer cells to cisplatin by directly targeting ABCC2. *Am J Transl Res* 9(3):1127-1138.
- To KK, Robey RW, Knutsen T, Zhan Z, Ried T and Bates SE (2009) Escape from hsa-miR-519c enables drug-resistant cells to maintain high expression of ABCG2. *Mol Cancer Ther* 8(10):2959-2968.
- van der Schoor LW, Verkade HJ, Kuipers F and Jonker JW (2015) New insights in the biology of ABC transporters ABCC2 and ABCC3: impact on drug disposition. *Expert Opin Drug Metab Toxicol* 11(2):273-293.
- Waetzig V, Haeusgen W, Andres C, Frehse S, Reinecke K, Bruckmueller H, Boehm R, Herdegen T, Cascorbi I (2019) Retinoic acid-induced survival effects in SH-SY5Y neuroblastoma cells. *J Cell Biochem* 120:5974-598.
- Werk AN, Bruckmueller H, Haenisch S, Cascorbi I (2014) Genetic variants may play an important role in mRNA-miRNA interaction: evidence for haplotype-dependent downregulation of ABCC2 (MRP2) by miRNA-379. *Pharmacogenet Genomics* 24:283-91.
- Yakusheva EN and Titov DS (2018) Structure and Function of Multidrug Resistance Protein 1. *Biochemistry (Mosc)* 83(8):907-929.
- Zhan M, Qu Q, Wang G and Zhou H (2013) Let-7c sensitizes acquired cisplatin-resistant A549 cells by targeting ABCC2 and Bcl-XL. *Pharmazie* 68(12):955-961.

Table 1: Sample and patient data

Donor ID	Tissue entity	Gender	Age	Diagnosis, TNM, Grade*
1	liver	m	63	hepatocellular carcinoma (HCC), pTxNxMx, G3
2	liver	f	69	HCC, pT3N1M0, G2
3	liver	m	74	HCC, pT3N0M0, G1
4	liver	m	68	liver metastasis of colon sigmoideum carcinoma, pT4N2M1, G3
5	liver	f	62	HCC, pT3aNxM1, G3
6	colon	m	77	colon sigmoideum, adenocarcinoma, pT3N0M0, G1
7	colon	f	75	colon ascendens, mucinous carcinoma, pT4N0M0, G3
8	colon	m	56	colon ascendens, adenocarcinoma, pT2N0M0, G2
9	colon	m	76	colon descendens, adenocarcinoma, pT3N2M1, G2
10	colon	m	71	cecum + colon ascendens, adenocarcinoma, pT4N0M0, G2
11	gall bladder	m	49	gall bladder, adenocarcinoma, pT2N0M0, G2
12	gall bladder	m	80	gall bladder, adenocarcinoma, pT4N2M0, G3
13	gall bladder	m	66	gall bladder, adenocarcinoma, pT3N0M1, G2
14	gall bladder	f	69	gall bladder, undifferentiated carcinoma, pT3NxMx, G4
15	gall bladder	f	75	gall bladder, adeno-squamous carcinoma, pT3N0M0, G3

*Please note that all tissues are peri-tumoral and non-malignant. TNM, TNM Classification of Malignant Tumors (TNM staging system); ID, identification

Table 2: Primer and primer specifications.

Primer name	Abbreviation*	Sequence 5'→3'	Position in gene
Reverse-Primer			
Poly-dT(RT)	RT	CCAGTGAGCAGAGTGACGAGGACTCGAGCTCAAGCT(n=17)	Poly-A-tail mRNA
Reverse (QO) 1	QO	CCAGTGAGCAGAGTGACG	Poly-dT(RT)
Reverse (QI) 2	QI	GAGGACTCGAGCTCAAGC	Poly-dT(RT)
Forward-Primer			
ABCC1			
ABCC1_F4568(-204)	C1-B	GACGACCTCATCCAGTCCAC	Exon 30
ABCC1_F4591(-181)	C1-A	CCGGACACAGTTCGAGGAC	Exon 30
ABCC1_F4884(113)	C1-F1	ACCAAACCCAGACAACCAAAAC	Exon 31
ABCC1_F4943(172)	C1-F2	CCTGGAAGTGGCTGTGAAGA	Exon 31
ABCC1_F5074(303)	C1-F3	TTCCCACGGAGGAGTTTTGG	Exon 31
ABCC1_F5204(433)	C1-F4	CTTCTGGCTCCCATCACCTC	Exon 31
ABCC1_F5368(597)	C1-F5	AGGCACTCAAAGCTGGGAA	Exon 31
ABCC1_F6045(1274)	C1-F6	TGATGCTCTTCCAGGACACG	Exon 31
ABCC1_F6197(1426)	C1-F7	GAGAAGCTCGCCCTGTGTT	Exon 31
ABCC1_Fgen6629(1858, 65)	C1-F8	TGTGGCATCTTCCTGTTTCTGT	Exon 31
ABCC1_Fgen6674(1903, 110)	C1-F9	CCTCTAGTGGGAGCTGTTGC	Exon 31
ABCC1_Fgen6727(1956, 163)	C1-F10	ATGGGGTTTAGTGGGAAGGC	Exon 31
ABCC2			
ABCC2_F4532(-354)	C2-B	GAAGTGACAGAGGCTGGTGG	Exon 30
ABCC2_F4642(-244)	C2-A	TGCGGTGGATCTAGAGACAGA	Exon 31
ABCC2_F4681(-205)	C2-F1	CATCCAAAACGAGTTCGCC	Exon 31
ABCC2_F4685(-201)	C2-F2	CAAACGAGTTCGCCACTG	Exon 31
ABCC2_F4761(-125)	C2-F3	TGGTCCTAGACAACGGGAAG	Exon 32
ABCC2_F4840(-46)	C2-F4	GGCTAAGGAAGCTGGCATTG	Exon 32

ABCC2_F5061(176)	C2-F5	TGAGAAACCCCTCGATTGTC	Exon 32
ABCC2_F5064(179)	C2-F6	GAAACCCCTCGATTGTCTACC	Exon 32
ABCC2_F5079(194)	C2-F7	TCTACCTCGATCGTACTTCCTTG	Exon 32
ABCC2_F5296(411)	C2-F8	TCATCCATGGTGATGCAAAT	Exon 32
ABCC3			
ABCC3_F4449(-217)	C3-B	CGACCTGGAGACTGACAACC	Exon 30
ABCC3_F4478(-188)	C3-A	CTACCATCCGCACCCAGTTT	Exon 30
ABCC3_F4630(-36)	C3-F1	TTCTACGGGATGGCCAGAGA	Exon 31
ABCC3_F4685(19)	C3-F2	CTCCTGGCCTTTCCTGGTTT	Exon 31
ABCC3_F4755(89)	C3-F3	CAAACACTGGGGGCACCTTA	Exon 31
ABCC3_F4844(178)	C3-F4	AAGTGGTGAATGACACGCCT	Exon 31
ABCC3_F4902(236)	C3-F5	GGTCTCCCGATTCCCAACTG	Exon 31
ABCC3_F5049(383)	C3-F6	AACAGAAGACAGCTGCTGGG	Exon 31
ABCC3_Fgen5194(530, 28)	C3-F7	TCACAAGGTTTGGGGATTAGGA	Exon 31
ABCC3_Fgen5315(651, 149)	C3-F8	ACAGCCAAAATTCCCTGGGT	Exon 31
ABCC3_Fgen5601(937, 435)	C3-F9	GTGTGAGCACAAAGAAGCCG	Exon 31
ABCC3_Fgen5882(1218, 716)	C3-F10	TCTCCCCAACCCCTAAATGGC	Exon 31
ABCC3_Fgen5965(1301, 799)	C3-F11	CTGTGCTGCAGGACCATTTG	Exon 31
ABCC3_Fgen6105(1441, 939)	C3-F12	CTGCCTCTCCTTGGTGCTAA	Exon 31
ABCC3_Fgen6107(1443, 941)	C3-F13	GCCTCTCCTTGGTGCTAAGA	Exon 31
ABCC3_Fgen6193(1529, 1027)	C3-F14	TAGCTGGCCTGAACCAACAG	Exon 31

* Referred to Fig. 1

Table 3: Micro-RNAs that have been reported and confirmed by luciferase reporter-gene assays to bind to the 3'-UTRs of *ABCC1*, *ABCC2*, and *ABCC3*.

mRNA	Micro-RNA	Reference
<i>ABCC1</i>	miR-7	(Hu et al., 2018; Liu et al., 2015)
	miR-9	(Sun et al., 2017)
	miR-133a	(Ma et al., 2015)
	miR-133b	(Chen et al., 2017)
	miR-185-5p	(Pei et al., 2016)
	miR-210-3p	(Li et al., 2018a)
	miR-326	(Liang et al., 2010)
	miR-1268a	(Li et al., 2018b)
	miR-1291	(Pan et al., 2013)
<i>ABCC2</i>	let-7c	(Zhan et al., 2013)
	miR-205-5p	(He et al., 2017)
	miR-379	(Haenisch et al., 2011)
	miR-490-3p	(Tian et al., 2017)
<i>ABCC3</i>	miR-143	(An et al., 2018)
	miR-192-5p	(Bruckmueller et al., 2017)

Legends to figures

Figure 1: *Schematic representation of all forward primers used in the present study.*

The numbers in the primer names specify the first nucleotide of their binding site within ABCC1 (at the top), ABCC2 (in the middle) and ABCC3 (at the bottom). The 3'-UTR is shown in dark grey, the CDS upstream the 3'-UTR and the genetic sequence downstream the 3'-UTR is shown in light grey. Additional sequence position information is shown at the top of ABCC1, ABCC2 and ABCC3 (end of CDS, start and end of the respective 3'-UTR according to NCBI, and the accession numbers of mRNA and gene sequences). Primers named with "gen" bind in genomic regions behind the given 3'-UTR (NCBI database) to observe if longer unknown 3'-UTRs exists in the respective mRNA.

Figure 2: *3'-RACE and agarose gel electrophoresis.*

Agarose gels are shown which resulted or partly resulted in evaluable ABCC1/ABCC2/ABCC3 3'-UTR sequences with a visible poly-A-tail. Arrows indicate gel extracted and sequenced amplicons. A white arrow indicates that sequencing of the respective amplicon resulted in evaluable ABCC1/ABCC2/ABCC3 3'-UTR sequences with a detectable poly-A-tail. Black arrows indicate artifacts (side products) unevaluable due to sequence overlays, or represent the expected sequence without a detectable poly-A-tail. If amplicons were generated in the first amplification round, this is noted at the bottom end of the gel. All other gel runs represent results generated with the second amplification round (nested PCR). In these cases, the respective primer combination used in the first amplification round is shown at the top of the gels. Primer combinations used to generate the amplicons are shown below the gels. A) Agarose gels of ABCC1, B) of ABCC2, and C) of ABCC3. Total RNA of the following

cell cultures was used as template: ABCC1: Lane 1, 2, 5, 6, 9, 10, 13, 14, 17, 18: SK-Hep-1; Lane 3, 4, 7, 8, 11, 12, 15, 16: Caco-2; ABCC2 (Lane 1-16) and ABCC3 (Lane 1-20): HepG2. M, marker (100 bp DNA ladder, Roth and 1 kb DNA ladder, Roth); ampl., amplification round

Figure 3: *Representation of the observed 3'-UTR variants of ABCC1, ABCC2, and ABCC3.*

3'-UTRs observed in the present study are shown in dark grey, a small part of the CDS upstream the 3'-UTR is shown in light grey. The start of the 3'-UTR is marked by an interrupted vertical line, the poly-A-tail is indicated by four A's. An asterisk at the indicated poly-A-tails suggest the most common 3'-UTR variant. The length of the observed 3'-UTRs is given within or right to the dark grey represented 3'-UTRs of the respective mRNAs.

Figure 4: *Proof of principle using luciferase reporter-gene assays applying three ABCC2 3'-UTRs and miR-379.*

The binding site of miR-379 within the ABCC2 3'-UTR is shown at the top. The upper diagram shows the results of the reporter-gene assay determined with miR-379 and the 178 bp ABCC2 3'-UTR variant (dark grey; no reduction of reporter-gene activity) compared to the 429 bp variant (light gray; concentration-dependent reduced reporter-gene activity) normalized to the negative control (black). The lower diagram shows the results determined with miR-379 and the 178 bp ABCC2 3'-UTR variant (dark grey; no reduction of reporter-gene activity) compared to the 944 bp variant (light gray; concentration-dependent reduced reporter-gene activity) normalized to the negative control (black). The Pre-miR™ miRNA Precursor Negative Control #1 (ThermoFisher Scientific) served as negative control, miR-379 was applied in three different

concentrations (10, 25, and 50 nM) as indicated below the diagrams. Data were analyzed using ANOVA and TukeyHSD post-hoc tests to detect statistically significant differences of (i) the negative control compared to different miR-379 concentrations and (ii) matching miR concentrations of the long and short fragments. Comparisons are indicated with horizontal lines on top, stars indicate significance (*= $p < 0.05$; **= $p < 0.01$, ***= $p < 0.001$). Error bars show +/- one standard deviation.

Figure 5: *Distribution of ABCC2 3'-UTR variants in human tissue.*

The binding regions of used primers pairs for qRT-PCR experiments are shown at the top. Three primer pairs were used with binding sites within the 178 bp, 363 bp, and 429 bp 3'-UTR variants of *ABCC2*. The relative expression to β -actin, normalized to the expression of the 178 bp 3'-UTR variant is shown for human liver (white), colon (light grey) and gall bladder samples (dark grey) as box whisker plots. Error bars depict minimum and maximum values. Data were analyzed using ANOVA with subsequent Tukey's post-hoc test; *, $p < 0.05$.

Figure 6: *ABCC2 protein quantification by immunoblotting and IOD calculation*

Western blots of *ABCC2* using gall bladder, liver and colon whole cell lysates and membrane enrichment of one respective liver sample are shown at the top. GAPDH was used as positive control. The calculated IOD (mean intensity optical densitometry) of *ABCC2* protein in the cell lysates normalized to GAPDH is shown at the bottom. In accordance to the antibodies datasheet (<https://datasheets.scbt.com/sc-518048.pdf>) and the literature *ABCC2* shows a size-variance in immunoblots probably due to posttranslational modifications. M, membrane fraction; C, cytosolic fraction.

Figure 7: *Detailed sequences with regulatory site tags and micro-RNA binding sites of ABCC1, ABCC2, and ABCC3.*

The stop codons are written in bold letters and are underlined at the beginning of each 3'-UTR. The binding sites of reported micro-RNAs for ABCC1 (at the top), ABCC2 (in the middle), and ABCC3 (at the bottom) are highlighted in light gray and the name of the respective micro-RNA is given below. Putative poly-A-signals and corresponding poly-A-sites are highlighted in dark grey. The length of the observed 3'-UTRs with ABCC1, ABCC2, and ABCC3 is given in brackets at every indicated poly-A-site.

Figure 1

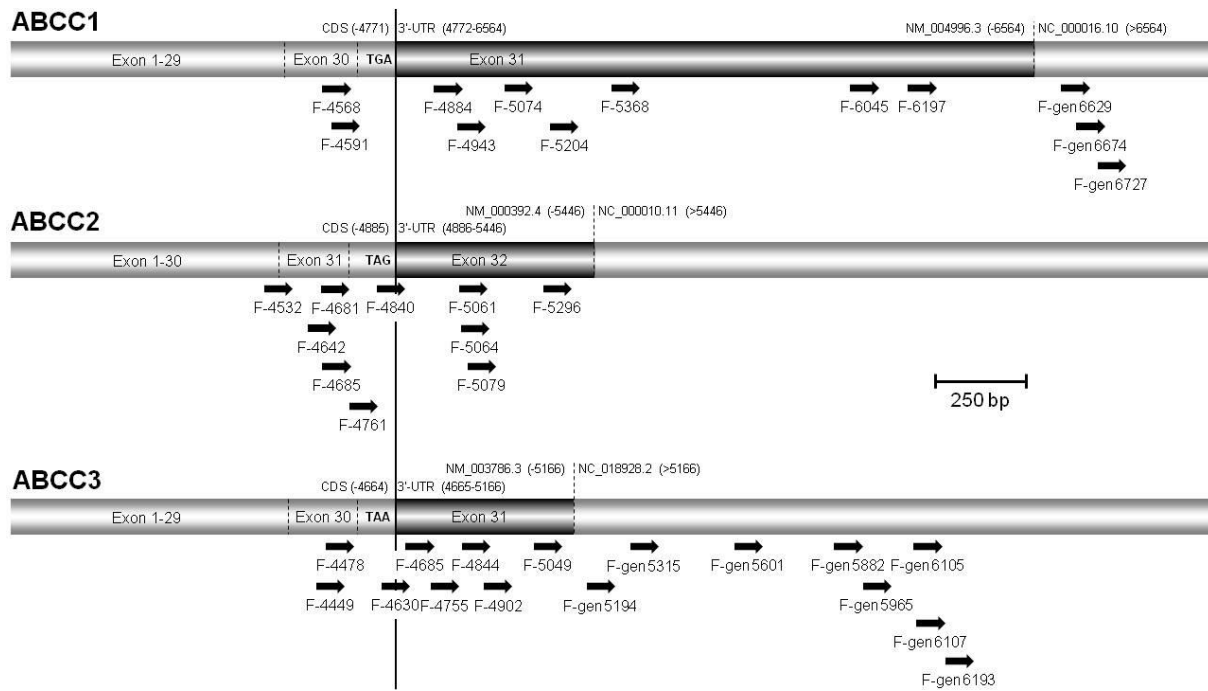
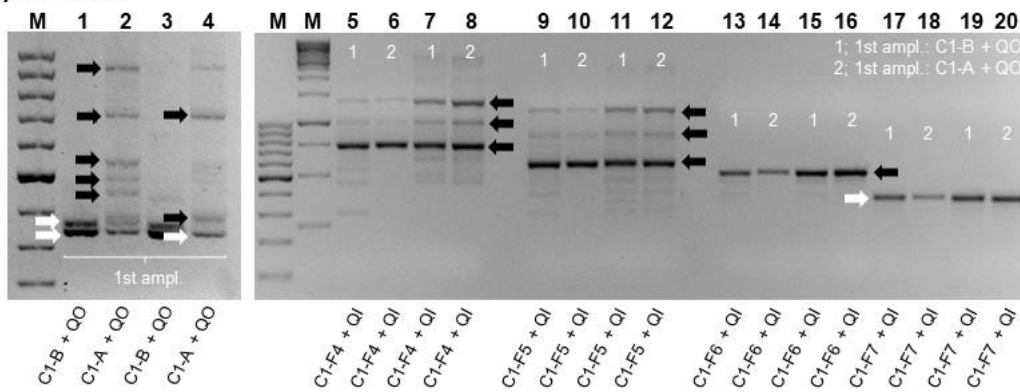
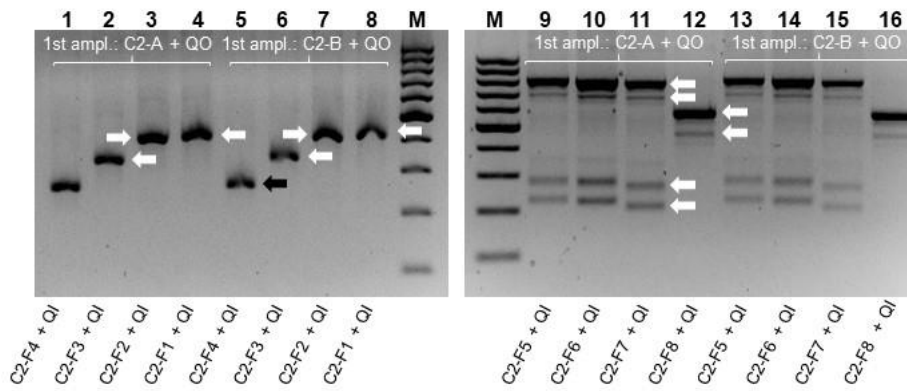


Figure 2

A) ABCC1



B) ABCC2



C) ABCC3

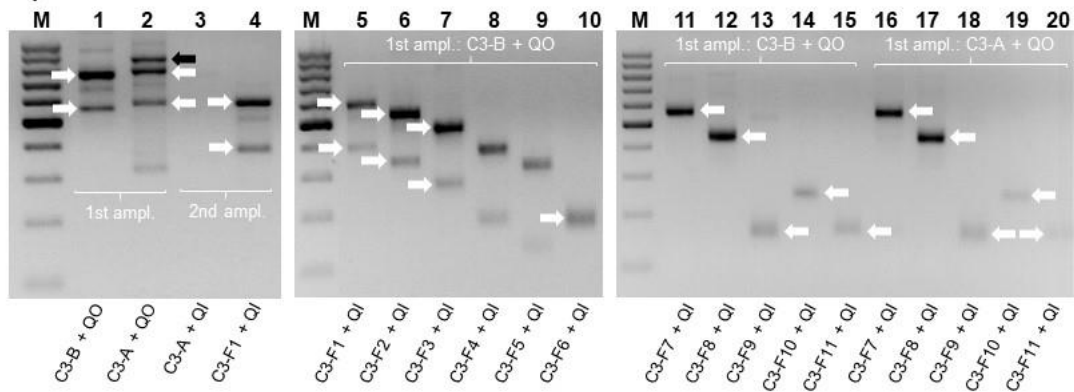


Figure 3

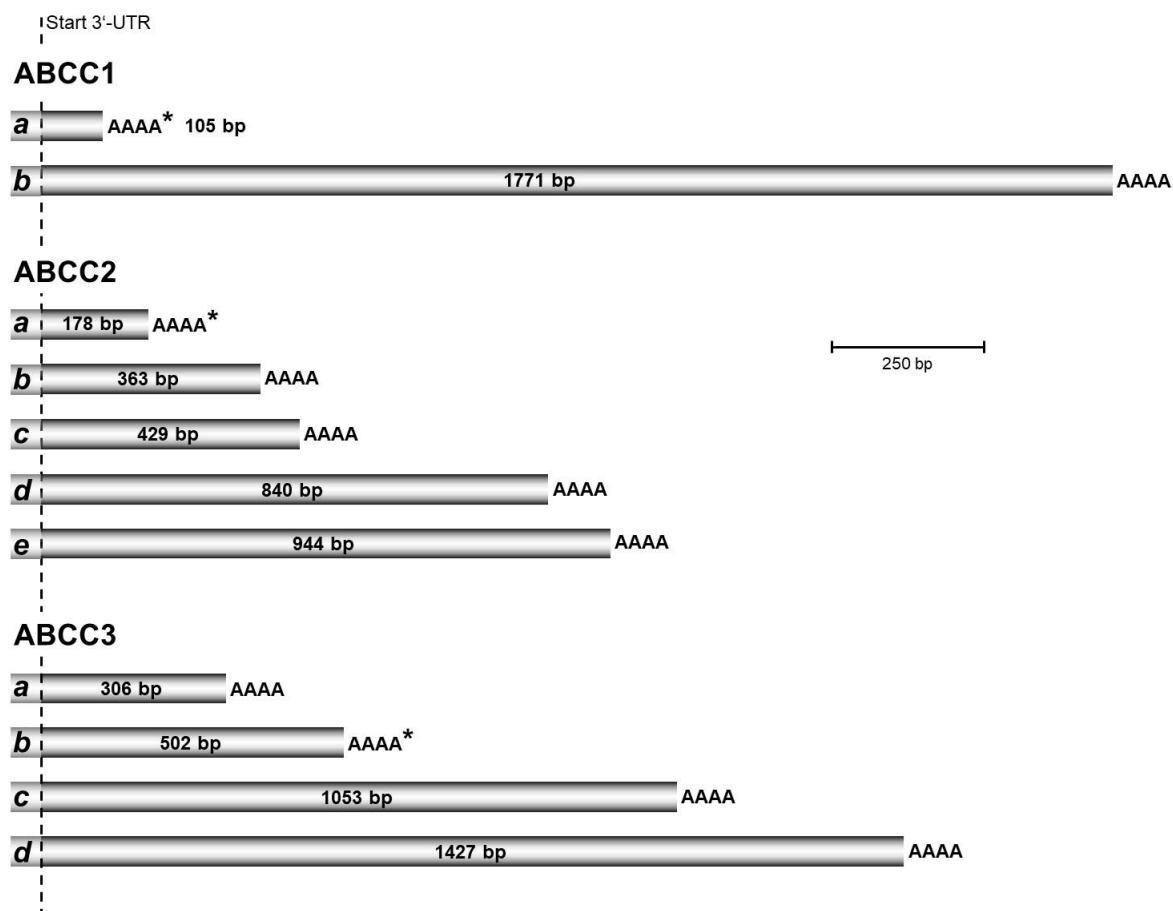


Figure 4

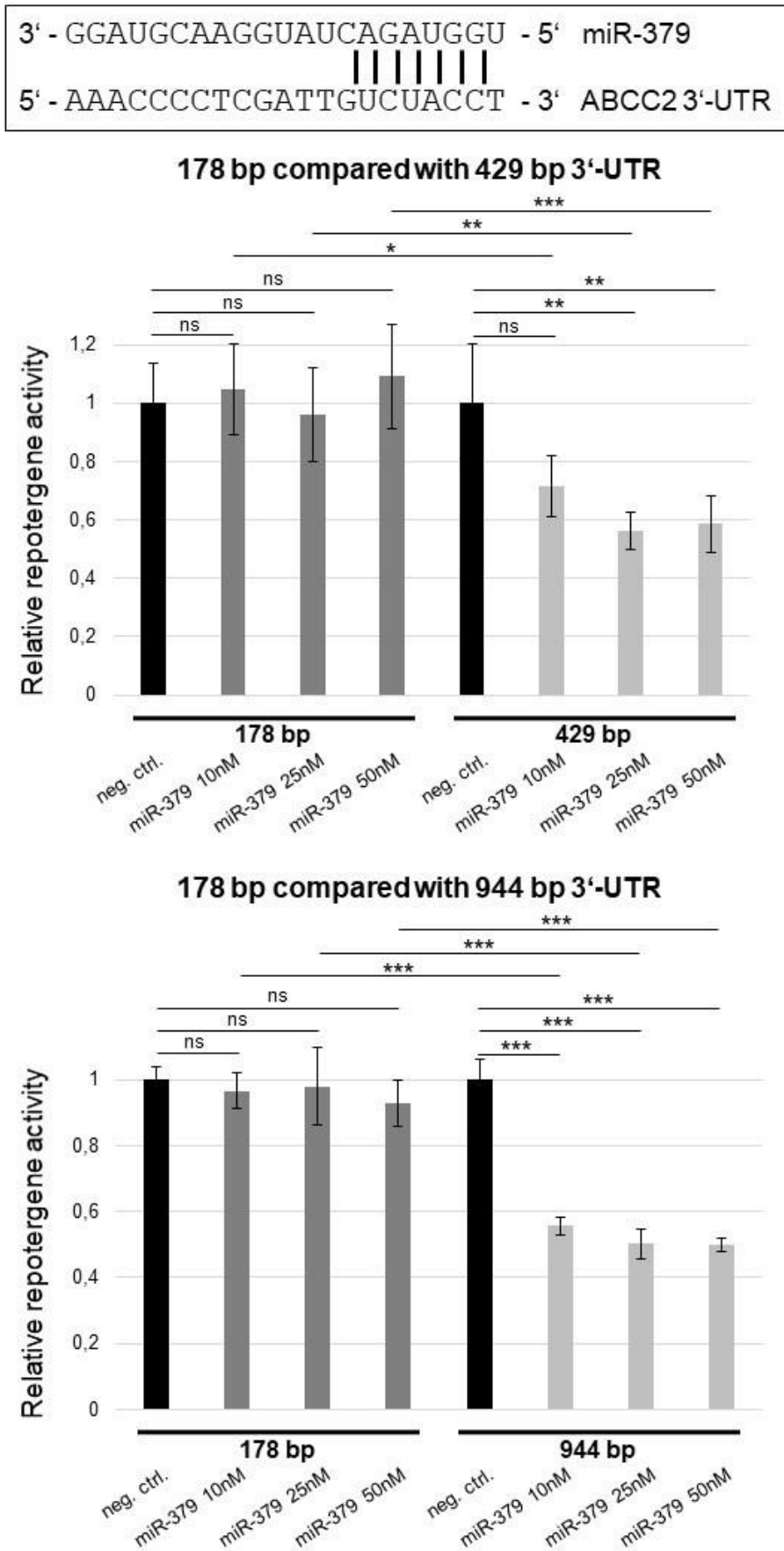


Figure 5

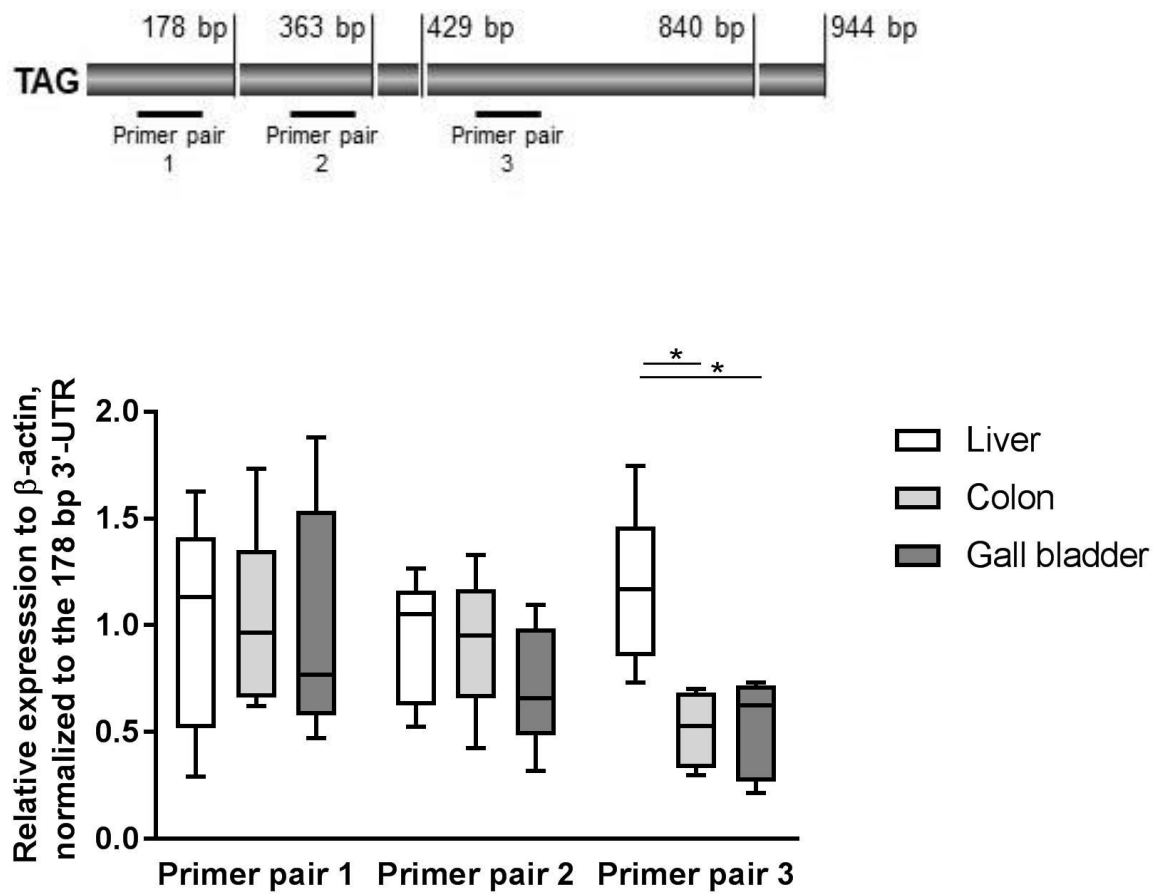


Figure 6

